Published Online: 2026 February 22 **Research Article**

Exploration of the Role of the lncRNA MALAT1 in Hepatic Alveolar Echinococcosis by Regulating the miR-378c/IGF1R Axis Via High-throughput Sequencing

Jinpeng Wang [1], Changzhen Shang [2], Zhen Liu [1], Zhigang Gai [1], Fucai Ma [1], Pan Xia [1], Yan Wang [3], Dewu Zhao [1], Hai-Hong Zhu [3,*]

[1] Department of Graduate School, Qinghai University, Xining, China
[2] Department of Hepatobiliary Surgery, Sun Yat-Sen Memorial Hospital, Guangzhou, China
[3] Department of General Surgery, Qinghai Provincial People's Hospital, Xining, China

[*] ***Corresponding Author:*** Department of General Surgery, Qinghai Provincial People's Hospital, Xining, China. Email: zhuhaihong1214@126.com

Received: 8 October, 2025; **Revised:** 27 December, 2025; **Accepted:** 7 February, 2026

Abstract

Background: Hepatic alveolar echinococcosis (HAE) is a severe parasitic disease with invasive growth characteristics similar to those of malignant tumors, and most patients cannot be cured by surgery. The drug treatment options are limited. Long non-coding RNAs (lncRNAs) and microRNAs (miRNAs) play key regulatory roles in the progression of various diseases, including liver cancer. The functions of molecules such as lncRNA metastasis-associated lung adenocarcinoma transcript 1 (MALAT1) and miR-378c in cancer have been widely reported, but their roles in HAE remain unclear.

Objectives: This study aims to identify aberrant lncRNAs as diagnostic biomarkers for the progression of hepatic alveolar echinococcosis through RNA sequencing (RNA-seq), and to investigate the potential mechanisms underlying lncRNA dysregulation in the advancement of this disease.

Methods: This paired-tissue study used RNA-seq (discovery set) on hepatic alveolar echinococcosis lesion tissues and matched adjacent liver tissues from three patients, followed by independent cohort validation by quantitative real-time polymerase chain reaction (qRT-PCR) (n = 20 for MALAT1 and insulin-like growth factor 1 receptor (IGF1R); n=13 for miR-378c). Lesion tissues from hepatic alveolar echinococcosis patients served as the experimental group, with adjacent tissues as controls. Metastasis-associated lung adenocarcinoma transcript 1 and IGF1R expression were further verified by qRT-PCR in lesion tissues and in liver tissues less than 1 cm and greater than 1 cm from the lesion. Meanwhile, miR-378c expression was assessed in a subset of patients. Potential binding sites among MALAT1, miR-378c, and IGF1R were predicted using StarBase and validated by dual-luciferase reporter assays.

Results: A total of 914 significantly differentially expressed lncRNAs were screened by RNA-seq in three samples of hepatic alveolar echinococcosis lesion tissues and adjacent tissues. Quantitative real-time polymerase chain reaction verification revealed that MALAT1 and IGF1R were highly expressed and that the level of miR-378c was low in hepatic alveolar echinococcosis lesions. A dual-luciferase assay revealed that MALAT1 targeted miR-378c and miR-378c targeted IGF1R in the three cases of hepatic alveolar echinococcosis. Differential expression was analyzed using DESeq2 with Benjamini–Hochberg false discovery rate (FDR) correction (FDR < 0.05, $|\text{fold change (FC)}| > 2$). In the validation cohort, qRT-PCR confirmed that MALAT1 and IGF1R were significantly upregulated whereas miR-378c was significantly downregulated in lesion tissues ($P < 0.05$). Correlation analysis showed that MALAT1 was negatively associated with miR-378c and positively associated with IGF1R, and miR-378c was negatively associated with IGF1R.

Conclusions: LncRNA MALAT1 may be involved in the progression of hepatic alveolar echinococcosis by acting as a molecular sponge for miR-378c and regulating the expression of the downstream target gene IGF1R.

Keywords: Hepatic Alveolar Echinococcosis, RNA-seq, lncRNA MALAT1, miR-378c, IGF1R

How to Cite: Wang J, Shang C, Liu Z, Gai Z, Ma F, et al. Exploration of the Role of the lncRNA MALAT1 in Hepatic Alveolar Echinococcosis by Regulating the miR-378c/IGF1R Axis Via High-throughput Sequencing. Hepat Mon. 2026;26(1):e166809. doi: https://doi.org/10.5812/hepatmon-166809

1. Background

Zoonosis caused by tapeworms of the genus *Echinococcus* is known as echinococcosis (1). This disease has become a serious public health problem by causing a large number of economic losses (2). Once swallowed, *Echinococcus* eggs make their way to the duodenum, where more than 70% head straight for the portal venous system before getting stuck in the liver. In this environment, they mature into cysts and create hepatic hydatid lesions. Hepatic echinococcosis can take over the entire liver, disrupting its anatomical structure and compromising its ability to function properly (3). Therefore, the organ most commonly targeted in echinococcosis is the liver (1). Radiologically and clinically, hepatic alveolar echinococcosis (HAE) resembles malignant tumors (4). Hepatic alveolar echinococcosis can infiltrate adjacent tissues such as the gallbladder and biliary system, as well as distant organs including the kidneys, lungs, and bones (5). At present, the treatment of HAE mainly includes surgery and drug therapy. Radical resection is the preferred treatment for HAE patients (6), but approximately 98% of patients cannot tolerate surgical treatment for various reasons (7). Many patients with HAE consequently lose surgical treatment options, making medical therapy their only option. However, the drug treatment cycle of echinococcosis is long, and specific drugs are still lacking. Recent research indicates that mmu-miR-342-3p likely stimulates hepatic stellate cell activation through ZBTTB7A-dependent TGF-β pathways in HAE (8). However, data on novel biomarkers of HAE are still scarce. Consequently, investigating fundamental molecular processes is essential.

RNA molecules exceeding 200 nucleotides that do not encode proteins are termed long non-coding RNAs (lncRNAs) (9). Although lncRNAs lack the ability to encode proteins, they are transcribed by at least 80% of mammals (10), and lncRNAs modulate diverse cellular functions, encompassing nuclear architecture and transcriptional plus posttranscriptional control of genes (11). In addition, lncRNAs act as "microRNA (miRNA) sponges" to disrupt the expression of target miRNA-mediated mRNAs, thereby acting as competing endogenous RNAs (ceRNAs) in the regulatory network (12). To date, more than 50,000 human lncRNAs have been identified (13). Metastasis-associated lung adenocarcinoma transcript 1 (MALAT1) stands out as one of the most extensively examined lncRNAs in the scientific community. Predominantly localized in the nucleus (14), this molecular player has its genomic coordinates pinned down to human chromosome 11q13.1, boasting a sequence length of roughly 8.7 kb (15). Research indicates it serves a critical function within many malignant tumors, mainly by regulating cancer cell proliferation, migration, and invasion (16). Among them, MALAT1 is closely related to hepatocellular carcinoma (HCC), and the progression of HAE is similar to that of HCC, suggesting that MALAT1 may have key functions in HAE similar to those in HCC. Unfortunately, the precise functions of MALAT1 in HAE are largely unknown.

MicroRNAs (miRNAs) represent a highly conserved family of non-coding RNA molecules, each approximately 18 - 25 nucleotides in length. These tiny but potent genetic regulators control gene expression by binding to complementary sequences within the 3' untranslated region (3'UTR) of target mRNAs. When they bind to these sites, they effectively suppress the target genes' expression, leading to reduced protein production through mRNA degradation (17). MiRNAs undergo a series of processing stages in the nucleus and cytoplasm (18). Recent investigations have shown that miRNAs are key players in cancer pathogenesis, by virtue of their ability to manipulate signaling pathways (19), regulate gene expression (20), and orchestrate fundamental biological processes like cell proliferation, mitosis, programmed cell death, and homeostatic balance (21) — collectively underscoring their integral role in both the initiation and progression of malignant diseases. According to relevant studies, miR-378c is related to many cancers via many miRNAs. For example, Hu and Luo (22) demonstrated that lnc-NORAD enabled miR-378c to inhibit gastric cancer progression through in vitro and in vivo studies. Therefore, it is necessary to further explore the relationship between miR-378c and HAE.

Although the role of MALAT1 in cancer progression and metastasis has been extensively studied, its function in patients with hepatic alveolar echinococcosis (HAE) has not been reported to our knowledge. Given the similarity between HAE and HCC in terms of invasive growth, we hypothesize that MALAT1 and its associated molecular network may play a similarly critical role in the pathogenesis of HAE. Therefore, this study aims to screen abnormally expressed lncRNAs in HAE via RNA sequencing (RNA-seq) and focus on investigating the potential mechanism of action of the MALAT1/miR-378c/insulin-like growth factor 1 receptor (IGF1R) regulatory axis in HAE progression.

2. Objectives

This study aims to identify aberrant lncRNAs as diagnostic indicators for the progression of hepatic alveolar echinococcosis through RNA-seq, and to investigate the potential mechanisms underlying lncRNA dysregulation in the advancement of this disease.

3. Methods

3.1. Patients and Samples

This study included 20 inpatients with HAE treated at Qinghai Provincial People's Hospital from September 2020 to December 2023. The hepatic hydatid lesion tissue was defined as the experimental group, while the surrounding hepatic tissues within 1 cm and beyond 1 cm from the lesion were designated as the control group. The research adheres to the principle of informed consent, and all participating patients voluntarily enrolled in the study. All subjects gave written consent, with the research protocol sanctioned by Qinghai Provincial People's Hospital Ethics Committee (Approval No: 2021-32).

3.2. Histopathological Examination

Representative lesion and adjacent liver tissues were fixed in 10% neutral-buffered formalin, embedded in paraffin, sectioned (approximately 4 μm), and stained with hematoxylin and eosin (H&E) following standard protocols. Slides were reviewed independently by experienced pathologists to confirm the diagnosis of HAE and to document major histopathological features.

3.3. RNA Extraction and RNA Sequencing

We harvested total RNA from the tissue samples, subsequently evaluating both its integrity and purity through 1% agarose gel electrophoresis and analysis with a NanoPhotometer® spectrophotometer (IMPLEN, CA, USA), respectively. To determine the RNA concentration, we employed a Qubit® 3.0 fluorometer (Life Technologies, CA, USA). The Agilent 2100 RNA Nano 6000 assay kit (Agilent Technologies, California, USA) provided the final assessment of RNA integrity. For library construction, we took 3 μg of total RNA from each sample and removed ribosomal RNA using Ribo-Zero Gold Kits (Human/Mouse/Rat). The resulting mRNA underwent fragmentation before we synthesized first-strand cDNA with random hexamers. The second strand was synthesized using dNTPs (including dUTP), RNase H, and DNA polymerase I. The cDNA libraries underwent purification using the QiaQuick PCR Kit, then received end repair, adenylation, adapter ligation, size selection through agarose gel electrophoresis, and were amplified by PCR. Library quality was assessed prior to pooling and sequencing on the Illumina platform (HiSeq/MiSeq). For reproducibility, we specify the reference genome and analysis pipeline as follows: Reads were aligned to the human reference genome [www.ncbi.nlm.nih.gov/datasets/genome/GCF_000001405.33/] using HISAT2. Gene-level counts were quantified using the count of sequencing reads in the transcript exon region and normalized in DESeq2. We also report sample-level quality control (QC) metrics (RIN values, total reads, sequencing depth, and mapping rates) in the revised Appendix 2.

3.4. RNA-Seq Raw Data Cleaning and Alignment

The raw genomic sequencing underwent quality control to minimize errors. Reads that did not meet the criteria (below a quality score of 20 and less than 35 base pairs in length) were excluded. Moreover, any bases scoring lower than 20 at the 3' end were trimmed. Reads containing Ns or falling below the length threshold after trimming were discarded. Uniquely mapped reads were utilized for gene read count and fragments per kilobase of transcript per million mapped reads (FPKM) calculations. Adjusted P-values (Benjamini–Hochberg) are reported for all differentially expressed lncRNAs (DElncRNAs).

3.5. Differentially Expressed Gene (DEG) Analysis

Differential expression analysis was performed using the DESeq2 software package in R Bioconductor. For the screening of DElncRNAs, we used the following criteria: The false discovery rate (FDR) corrected by the Benjamini–Hochberg method was less than 0.05, and the fold change (FC) was greater than 2.

3.6. Quantitative Real-time Polymerase Chain Reaction

RNA was isolated using the TRIzol Reagent (Ambion, Austin, Texas, USA) following the manufacturer's guidelines. cDNA was synthesized from 1 μg of total RNA using the 5X All-In-One RT MasterMix (ABM, Vancouver, Canada) for mRNAs/lncRNAs and a one-step miRNA cDNA synthesis kit (Genenode, Hubei, China) for miRNAs. The Quantitative real-time polymerase chain reaction (qRT-PCR) process was carried out with EvaGreen Express 2×qPCR MasterMix-Low Rox (ABM, Vancouver, Canada) for mRNAs/lncRNAs and miRNA SYBR Green qPCR Mix (Genenode, Hubei, China) for miRNAs. Relative expression levels were calculated

using the $2^{-\Delta\Delta Ct}$ method. Primer sequences are listed in Table 1.

Table 1. Primer Information for Quantitative Real-time Polymerase Chain Reaction

Name of Genes	Sequence (5′-3′)
lncRNA MALAT	
Forward	GGGTGTTTACGTAGACCAGAACC
Reverse	CTTCCAAAAGCCTTCTGCCTTAG
IGF1R	
Forward	GAGAGGAGCAGCTAGAAGGG
Reverse	CCCTTTAGTCCCCGTCACTT
miR-378c	
Forward	TGGCCAGGGAGCAG
Reverse	GTTTTTTTTTTTTTTCCCACCAG

3.7. Cell Culture and Transfection

The 293T human embryonic kidney cell line was obtained from Pronosai Bio. The cell medium was DMEM (GIBCO, Grand Island, NY, USA) supplemented with 10% fetal bovine serum (Excell Bio, JiangSu, China). 1% penicillin–streptomycin double antibody (10000 U) (GIBCO, Grand Island, NY, USA) was used. The cell lines were maintained at 37°C in a humidified incubator containing 5% CO_2. MALAT1 (si-MALAT1), the miR-378c mimic (miR-378c), the negative control (NC), and IGF1R (si-IGF1R) were synthesized by Ubao Bio (Hunan, China). The transfection process was carried out using Lipofectamine® 3000 (Invitrogen, Carlsbad, CA, USA) according to the provided protocol. A 48-hour incubation period was allowed before the cells were processed for subsequent experimental analyses. To preliminarily explore the biological functions of the MALAT1/miR-378c/IGF1R axis, we transfected it into LX-2 cells. Cell proliferation was detected using the CCK-8 assay kit, and cell migration ability was evaluated using a Transwell chamber (8.0 μm pore size, Corning). Please refer to the manufacturer's instructions for specific procedures.

3.8. Luciferase Reporter Assay

To investigate possible interactions involving MALAT1, we used StarBase (http://starbase.sysu.edu.cn/index.php) and verified that MALAT1 and miR-378c had complementary binding sites. To identify potential downstream targets of miR-378c, we utilized StarBase and identified IGF1R as one such target. Following transfection of the constructed wild-type or mutant reporter plasmids along with miR-378c mimic or negative control into HEK-293T cells or LX-2 cells and adhering to the manufacturer's guidelines, we discarded the culture medium and introduced 75 μL of premixed Dual-Glo® Luciferase Reagent (Promega, Madison, WI, USA) to each sample. They were then transferred to 96-well luciferase plates (75 μL of cell suspension per well). Firefly luciferase fluorescence values were measured within 2 hours via a fluorescence microplate reader (Thermo Fisher, Waltham, MA, USA). Subsequently, 75 μL of premixed Dual-Glo® Stop & Glo® Reagent (Promega, Madison, WI, USA) was added to each well, allowed to stand for 5 minutes, and Renilla luciferase fluorescence was measured. Luciferase activity is represented as the quotient of firefly luminescence intensity relative to Renilla luminescence intensity.

3.9. Statistical Analysis

Data are presented as mean ± standard deviation. Statistical analysis was performed using SPSS 28.0 software. One-way analysis of variance (ANOVA) was used for comparisons among multiple groups, and the least significant difference (LSD) test was applied for pairwise comparisons between groups. Spearman correlation analysis was used to assess the correlations between MALAT1 and miR-378c, as well as between MALAT1 and IGF1R. Pearson correlation analysis was employed to evaluate the correlation between miR-378c and IGF1R. Data from cell function experiments were compared using the *t*-test. A P value < 0.05 was considered statistically significant.

4. Results

4.1. Transcriptome Sequencing of HAE Tissues and Identification of Differentially Expressed LncRNAs

To investigate the characteristics of novel transcripts in HAE, we conducted sequencing analyses on lesional tissues and adjacent non-lesional tissues from three HAE patients. A total of 130,000 lncRNA raw sequences were obtained, with Q30 scores exceeding 90% across all samples, indicating high sequencing quality (Appendix 1 in Supplementary File for details). We evaluated RNA-seq data quality through inter-sample correlation analysis (Figure 1A) and principal component analysis (PCA; Figure 1B). These analyses revealed a strong correlation between HAE lesion and adjacent tissues in all three patients. This research revealed 2,140 lncRNAs were identified in HAE tissues and adjacent liver tissue samples by RNA-seq. According to the set screening criteria (FDR < 0.05 and FC > 2), we identified 914 significantly differentially expressed lncRNAs (648 upregulated and 266 downregulated) among the 2,140

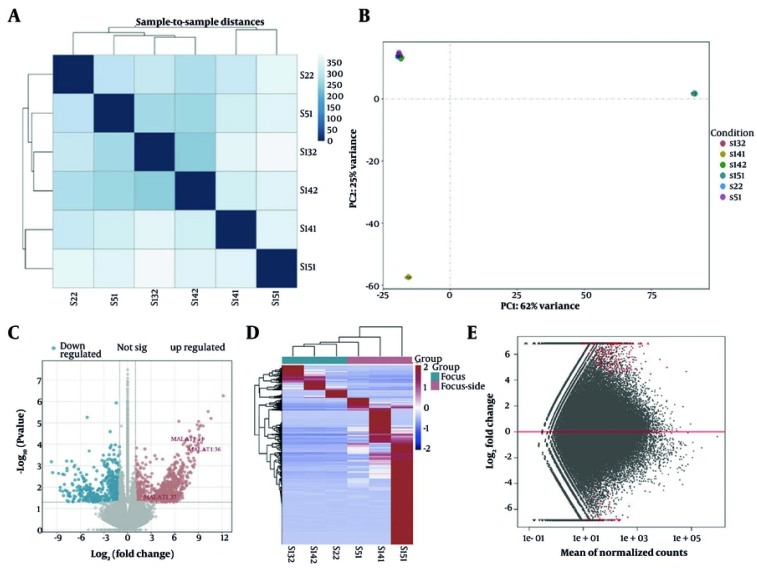

Figure 1. Analysis of sequencing data and Identification of differentially expressed lncRNAs between HAE lesion tissue and HAE paralesion tissue. A, Sample correlation heatmap of lncRNA expression in sequenced samples; B, PCA of lncRNAs based on sequenced samples; C, differential gene volcano plot of differentially expressed lncRNAs in the HAE sequencing data. The red dots represent the upregulated RNAs, and the blue dots represent the downregulated RNAs. The grey dots indicate RNAs whose expression was not significantly different; D, heatmap of differentially expressed lncRNAs in the HAE sequencing data; E, MA plot of differentially expressed lncRNAs in the HAE sequencing data.

lncRNAs (Figure 1C). Moreover, the heatmap revealed that the lncRNAs in the HAE tissues were well distinguished from those in the HAE-adjacent tissues (Figure 1D). In addition, the findings from the lncRNA differential expression study are depicted in Figure 1E.

4.2. Quantitative Real-time Polymerase Chain Reaction detection

Quantitative real-time polymerase chain reaction revealed a substantial increase in MALAT1 expression within HAE tissue samples, when contrasted with surrounding (< 1 cm) and distant (> 1 cm) liver sections (Figure 2A). In stark contrast, miR-378c showed significantly diminished expression in the focal tissues of HAE patients (Figure 2B). These results indicate that MALAT1 is highly expressed and that miR-378c is expressed at low levels in the focal tissues of hepatic alveolar echinococcosis patients. Correlation analysis revealed a negative correlation between MALAT1 expression levels and miR-378c levels in HAE lesions (Figure 2C).

4.3. Metastasis-Associated Lung Adenocarcinoma Transcript 1 is a Direct Target of miR-378c

Drawing from the competing endogenous RNA (ceRNA) hypothesis, we set out to examine whether MALAT1 and miR-378c might be able to interact. Bioinformatic analysis via StarBase predicted potential complementary binding sequences between these two molecules (Figure 3A). Next, to further verify the complementary binding relationship between the two genes, we performed a dual-luciferase reporter assay to investigate their interaction. Subsequently, wild-type (MALAT1-WT) and mutant (MALAT1-MT) plasmids containing miR-378c binding sites were constructed as dual-luciferase reporter genes. The dual-luciferase assays clearly showed that MALAT1-WT cells exhibited markedly reduced luciferase activity compared to MALAT1-NC cells that had been transfected with miR-378c in both HEK-293T and LX-2 cells. On the other hand, the luciferase readings from MALAT1-MT cells remained largely unaffected by the transfection process (Figure 3B). These results strongly support our hypothesis that MALAT1 directly binds to miR-378c.

4.4. miR-378c Directly Targets and Binds to IGF1R

To further investigate the downstream targets of miR-378c in HAE cells, bioinformatics analysis (StarBase) predicted IGF1R, a gene implicated in metastasis and

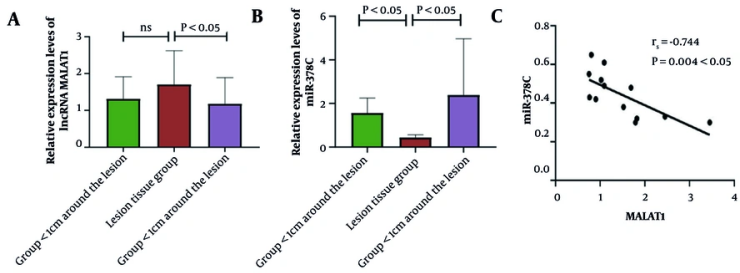

Figure 2. A, Bar chart of lncRNA MALAT1 expression levels in each group; B, bar chart of miR-378c expression levels in each group; and C, correlation between MALAT1 levels and miR-378c levels in HAE patients.

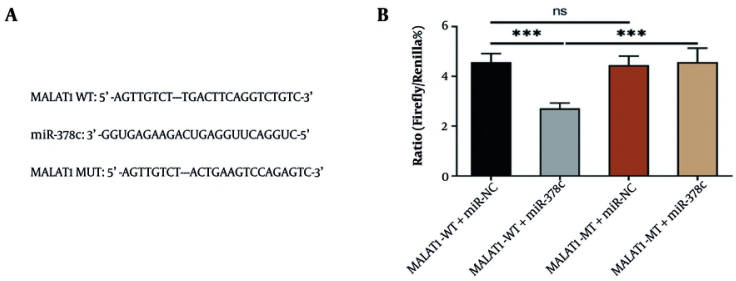

Figure 3. A, Complementary binding sites between MALAT1 and miR-378c; B, bar graph of the dual luciferase activity assay results for MALAT1 and miR-378c (*** $P < 0.001$).

studied in various tumors, as a prime candidate for miR-378c, complete with complementary binding regions (Figure 4A). Quantitative real-time polymerase chain reaction confirmed elevated IGF1R expression in HAE lesions compared to control tissues (Figure 4B). Further analysis revealed that IGF1R expression demonstrated a positive correlation with MALAT1 while maintaining an inverse relationship with miR-378c (Figure 4D and E); therefore, we hypothesized that IGF1R may be regulated by miR-378c in HAE cells. Next, we conducted a dual-luciferase assay for confirmation. Wild-type (IGF1R-WT) and mutant (IGF1R-MT) plasmids containing miR-378c binding sites were constructed as dual-luciferase reporter genes. The results showed that compared with IGF1R-NC-transfected cells, the luciferase value of IGF1R-WT-transfected cells decreased significantly in both HEK-293T and LX-2 cells, but the fluorescence value of IGF1R-MT-transfected cells remained largely unchanged (Figure 4C). Synthesizing these findings, it is clear that miR-378c has a direct binding affinity for IGF1R mRNA, potentially modulating its expression within HAE patient cell cultures.

4.5. Preliminary Validation of Functional Assays

To explore the potential biological significance of the MALAT1/miR-378c/IGF1R axis, we performed functional experiments in LX-2 cells. The results showed that, compared with cells transfected with negative controls, knockdown of MALAT1 (si-MALAT1) or overexpression of miR-378c (miR-378c mimic) significantly inhibited the proliferation and migration capabilities of LX-2 cells. Similarly, knockdown of IGF1R (si-IGF1R) also produced comparable inhibitory effects on cell proliferation and migration.

4.6. Histopathological Features of HAE Lesions

Histopathological examination confirmed the diagnosis of hepatic alveolar echinococcosis in lesion tissues and demonstrated characteristic lesion architecture and host inflammatory responses.

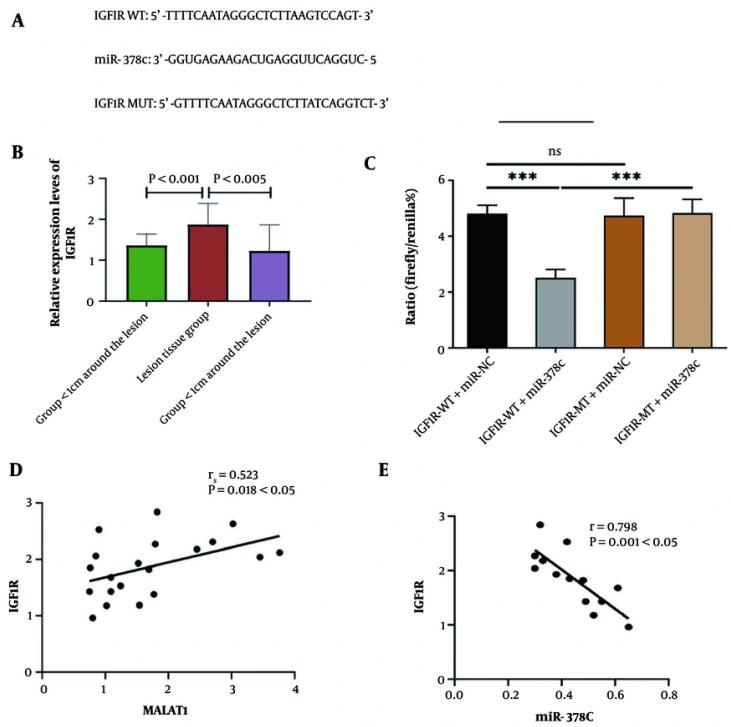

Figure 4. A, Complementary binding sites exist between IGF1R and miR-378c; B, bar chart of the IGF1R expression level in each group; C, bar chart of miR-378c and IGF1R dual luciferase activity detection. (D) Correlation between the IGF1R and MALAT1 levels in HAE patients. E, Correlation between the IGF1R and miR-378c levels in HAE patients (*** P < 0.001).

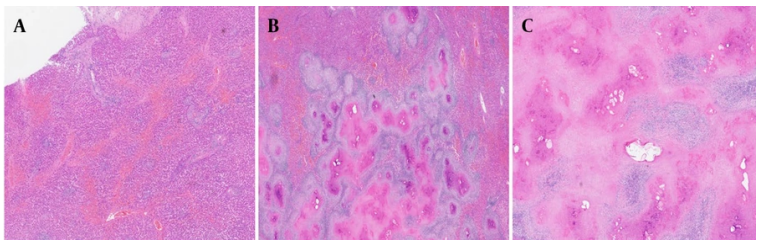

Figure 5. A, Histopathological image of normal liver tissue; B, histopathological image of adjacent liver tissue; C, histopathological image of lesional tissue.

Representative H&E images of lesion and adjacent liver tissues are provided in Figure 5.

5. Discussion

Human echinococcosis mainly occurs in the liver, emerging as a dangerous parasitic condition with hepatic origins. HAE is called "cancer of worms" (6). Studies have shown that as tapeworms proliferate within their host's liver, there is always a molecular-level interaction between the host and the parasite (23). IGF1R is a central mediator of growth-factor signaling in the liver and has been implicated in hepatocyte survival, hepatic stellate cell activation, and fibrogenic remodeling in chronic liver injury. Although direct

evidence in parasitic liver diseases remains limited, persistent inflammatory stimulation and tissue remodeling in HAE may converge on IGF1R-related pathways, which provides a biologically plausible context for our observation that IGF1R expression is elevated in HAE lesions and inversely associated with miR-378c. We have revised the Discussion to emphasize that these findings indicate an association and support a testable mechanistic hypothesis for future work.

Currently, many studies have reported the regulation of lncRNAs in hepatocellular carcinoma, but research on HAE is still largely lacking. According to Tuergan et al. (24), nanosecond pulsed electric field therapy can effectively curb lesion progression and modify gene expression patterns within HAE tissues, some of which are regulated by lncRNAs. Therefore, exploring lncRNAs and their biological functions may provide important new impetus for HAE research and treatment. To shed light on the biological significance of lncRNAs in HAE and discover new transcripts in HAE, we selected three HAE lesion tissues and paralesion liver tissues for RNA-seq and transcriptome analysis in strict accordance with the inclusion and exclusion criteria.

In the present investigation, we employed RNA-seq to profile lncRNA expression in HAE lesion and paralesion tissues. We identified 914 differentially expressed lncRNAs, with 648 upregulated and 266 downregulated. Through high-throughput sequencing, we found that MALAT1 was significantly differentially expressed and upregulated in HAE lesions. To pinpoint regulatory RNAs linked to observable clinical manifestations, we constructed a ceRNA network for HAE by integrating miRNA-targeted lncRNA and mRNA analyses. Based on this framework, we hypothesize that MALAT1 may contribute to HAE pathogenesis through regulating the miR-378c/IGF1R axis.

Among numerous lncRNAs, MALAT1 first came to light as a prognostic indicator for early-stage lung adenocarcinoma (25). Metastasis-associated lung adenocarcinoma transcript 1 is a classical lncRNA capable of targeting genes through both direct regulation of gene expression and indirect manipulation of miRNAs, playing a pivotal role in tumor migration, invasion, and proliferation across various cancer types (26). For example, in glioblastoma, the MALAT1–miR-199a–ZHX1 pathway acts as a driving force behind the multiplication and advancement of the malignancy (27). Currently, many studies have linked MALAT1 to cancer progression and metastasis. However, to our knowledge, MALAT1 has not been studied in HAE patients until now. Consistent with previous studies, high-throughput sequencing revealed that MALAT1 was upregulated in HAE lesion tissues, which was further confirmed by qRT-PCR, and its expression increased with proximity to the lesion. Therefore, we conjecture that MALAT1 might be intricately tied to the onset and progression of HAE, and its mechanism in HAE may be similar to its function in cancer.

Research has increasingly demonstrated that miRNAs are key regulators in parasitic and chronic liver diseases (28). Cai et al. (29) identified several miRNAs — including miR-21, miR-34a, and miR-122 — as promising candidates for early schistosomiasis detection. This evidence strongly suggests that aberrant miRNA expression can predict the occurrence and development of parasitic diseases. miR-378c, a member of the miR-378 family located on chromosome 10q26.3 (22), was found to be downregulated in HAE lesions in our study, with decreasing expression towards the lesion center. On the other hand, our dual-luciferase experiments demonstrated that MALAT1 directly engages with miR-378c. When we examined the MALAT1–miR-378c dynamic in HAE patients, an inverse correlation emerged, suggesting these molecules might be locked in a negative regulatory relationship. Therefore, we hypothesized that MALAT1 may negatively regulate miR-378c expression by serving as a molecular sponge for miR-378c in HAE.

Researchers know that miRNAs work by attaching themselves to the mRNAs of their subsequent targets, which either results in the mRNA's degradation or inhibits its translation process (30). We confirmed that IGF1R, a potential downstream target, is highly expressed in HAE lesions and positively correlates with MALAT1. The dual-luciferase assay verified that miR-378c directly targets IGF1R. The negative correlation between miR-378c and IGF1R expression, coupled with the positive correlation between MALAT1 and IGF1R, fits the ceRNA model: MALAT1 sequesters miR-378c, alleviating its repression of IGF1R, thereby increasing IGF1R expression. In conclusion, we found that miR-378c directly binds to and regulates IGF1R, and IGF1R may be associated with the progression of HAE.

In summary, we found that MALAT1 and IGF1R were highly expressed but that miR-378c was downregulated in the lesion tissues of HAE patients, which may be linked to the disease's onset and advancement. In addition, we revealed that MALAT1 may act as a molecular sponge for miR-378c, regulating the expression of the downstream target gene IGF1R, and thus may be involved in the metastasis and invasion of HAE cells. This newly identified MALAT1/miR-378c/IGF1R axis could be pivotal in the progression of HAE, offering

new insights into its molecular pathogenesis and potential avenues for future therapeutic strategies.

Supplementary Material

Supplementary material(s) is available here [To read supplementary materials, please refer to the journal website and open PDF/HTML].

Footnotes

AI Use Disclosure: The authors declare that no generative AI tools were used in the creation of this article.

Authors' Contribution: Study concept and design: Z. H. H, W. J. P, S. C. Z, L. Z., and G. Z. G; Acquisition of data: W. J. P., L. Z., G. Z. G., Z. D. W., and M. F. C.; Analysis and interpretation of data: W. J. P., L. Z., X. P., and G. Z. G.; Drafting of the manuscript: W. J. P.; Critical revision of the manuscript for important intellectual content: Z. H. H. and S. C. Z.; Statistical analysis: W. J. P., L. Z., and X. P.; Administrative, technical, and material support: Z. H. H., S. C. Z., and W. Y.; Study supervision: Z. H. H. and S. C. Z.

Conflict of Interests Statement: Z.H.H: Funding and research support from Qinghai Provincial Science and Technology Department (Project No. 2022-ZJ-747) and the KunLun Talents High-end Innovation and Entrepreneurship Talent Program of Qinghai Province (Youth Talent character [2021] No. 13); employment: Qinghai People's Hospital. No personal financial interests, consulting fees, patents, or relevant memberships. No editorial or reviewer role for this journal.

Data Availability: The data presented in this study are uploaded as a supplementary file during submission and are openly available to readers upon request [Dataset name: Supplementaly File]. The data are also openly available in Gene Expression Omnibus at https://www.ncbi.nlm.nih.gov/geo/query/acc.cgi? , reference number GSE267663.

Ethical Approval: This study was approved under the ethical approval code 2021SLCJ1588 .

Funding/Support: This research was supported in part by the Qinghai Provincial Science and Technology Department under the project "Research on differential expression of LncRNA and circRNA and related signalling pathways in hepatic alveolar echinococcosis" (Project No. 2022-ZJ-747), and the KunLun Talents High-end Innovation and Entrepreneurship Talent Program of Qinghai Province (Youth Talent character [2021] No. 13).

Informed Consent: Informed consent was obtained.

References

1. Hu Q, Chen S, Fan Y, Lu Q, Deng M, Fan H. Kidney invasion occurred 2 years following liver transplantation for hepatic alveolar echinococcosis: a case report. *BMC Infect Dis*. 2023;**23**(1):785. [PubMed ID: 37950231]. [PubMed Central ID: PMC10638689]. https://doi.org/10.1186/s12879-023-08788-7.
2. Kantarci M, Aydin S, Eren S, Ogul H, Akhan O. Imaging Aspects of Hepatic Alveolar Echinococcosis: Retrospective Findings of a Surgical Center in Turkey. *Pathogens*. 2022;**11**(2). [PubMed ID: 35215218]. [PubMed Central ID: PMC8877742]. https://doi.org/10.3390/pathogens11020276.
3. Wang YX, Liu W, Sun ZY, Wu L, Xie XK, Liu B. Analysis of Ultrasonographic Characteristics of Early Hepatic Alveolar Echinococcosis. *Front Surg*. 2022;**9**:918138. [PubMed ID: 35865038]. [PubMed Central ID: PMC9294286]. https://doi.org/10.3389/fsurg.2022.918138.
4. Akbulut S, Sahin TT. Comment on surgical approaches for definitive treatment of hepatic alveolar echinococcosis: results of a survey in 178 patients. *Parasitology*. 2020;**147**(13):1408-10. [PubMed ID: 32741385]. [PubMed Central ID: PMC10317737]. https://doi.org/10.1017/S0031182020001390.
5. Pavlidis ET, Galanis IN, Pavlidis TE. Current considerations for the management of liver echinococcosis. *World J Gastroenterol*. 2025;**31**(10):103973. [PubMed ID: 40093668]. [PubMed Central ID: PMC11886533]. https://doi.org/10.3748/wjg.v31.i10.103973.
6. A J, Chai J, Shao Z, Zhao S, Wang H, A X, et al. Comparison of local ablation with Albendazole or laparoscopic hepatectomy combined with Albendazole in the treatment of early hepatic alveolar echinococcosis. *Front Public Health*. 2022;**10**:960635. [PubMed ID: 36276387]. [PubMed Central ID: PMC9580460]. https://doi.org/10.3389/fpubh.2022.960635.
7. Ozdemir S, Aksungur N, Altundas N, Kara S, Korkut E, Ozkaraca M, et al. Genome-wide profiling of the expression of serum derived exosomal circRNAs in patients with hepatic alveolar echinococcosis. *Gene*. 2022;**814**:146161. [PubMed ID: 34995736]. https://doi.org/10.1016/j.gene.2021.146161.
8. Cao S, Wang D, Wu Y, Zhang J, Pu L, Luo X, et al. mmu-miRNA-342-3p promotes hepatic stellate cell activation and hepatic fibrosis induced by Echinococcus multilocularis infection via targeting Zbtb7a. *PLoS Negl Trop Dis*. 2023;**17**(7). e0011520. [PubMed ID: 37490505]. [PubMed Central ID: PMC10403128]. https://doi.org/10.1371/journal.pntd.0011520.
9. Li P, Ma X, Gu X. LncRNA MAFG-AS1 is involved in human cancer progression. *Eur J Med Res*. 2023;**28**(1):497. [PubMed ID: 37941063]. [PubMed Central ID: PMC10631199]. https://doi.org/10.1186/s40001-023-01486-9.
10. Park EG, Pyo SJ, Cui Y, Yoon SH, Nam JW. Tumor immune microenvironment lncRNAs. *Brief Bioinform*. 2022;**23**(1). [PubMed ID: 34891154]. [PubMed Central ID: PMC8769899]. https://doi.org/10.1093/bib/bbab504.
11. Malissovas N, Ninou E, Michail A, Politis PK. Targeting Long Non-Coding RNAs in Nervous System Cancers: New Insights in Prognosis, Diagnosis and Therapy. *Curr Med Chem*. 2019;**26**(30):5649-63. [PubMed ID: 30182849]. https://doi.org/10.2174/0929867325666180831170227.

12. Zhou Y, Zhou C, Wei L, Han C, Cao Y. The ceRNA Crosstalk between mRNAs and lncRNAs in Diabetes Myocardial Infarction. *Dis Markers*. 2022;**2022**:4283534. [PubMed ID: 35592708]. [PubMed Central ID: PMC9112177]. https://doi.org/10.1155/2022/4283534.
13. Iyer MK, Niknafs YS, Malik R, Singhal U, Sahu A, Hosono Y, et al. The landscape of long noncoding RNAs in the human transcriptome. *Nat Genet*. 2015;**47**(3):199-208. [PubMed ID: 25599403]. [PubMed Central ID: PMC4417758]. https://doi.org/10.1038/ng.3192.
14. Liu W, Wang Z, Liu L, Yang Z, Liu S, Ma Z, et al. LncRNA Malat1 inhibition of TDP43 cleavage suppresses IRF3-initiated antiviral innate immunity. *Proc Natl Acad Sci U S A*. 2020;**117**(38):23695-706. [PubMed ID: 32907941]. [PubMed Central ID: PMC7519350]. https://doi.org/10.1073/pnas.2003932117.
15. Hao L, Wu W, Xu Y, Chen Y, Meng C, Yun J, et al. LncRNA-MALAT1: A Key Participant in the Occurrence and Development of Cancer. *Molecules*. 2023;**28**(5). [PubMed ID: 36903369]. [PubMed Central ID: PMC10004581]. https://doi.org/10.3390/molecules28052126.
16. Sun Y, Ma L. New Insights into Long Non-Coding RNA MALAT1 in Cancer and Metastasis. *Cancers (Basel)*. 2019;**11**(2). [PubMed ID: 30781877]. [PubMed Central ID: PMC6406606]. https://doi.org/10.3390/cancers11020216.
17. Shi T, Morishita A, Kobara H, Masaki T. The Role of Long Non-Coding RNA and microRNA Networks in Hepatocellular Carcinoma and Its Tumor Microenvironment. *Int J Mol Sci*. 2021;**22**(19). [PubMed ID: 34638971]. [PubMed Central ID: PMC8508708]. https://doi.org/10.3390/ijms221910630.
18. Xu X, Tao Y, Shan L, Chen R, Jiang H, Qian Z, et al. The Role of MicroRNAs in Hepatocellular Carcinoma. *J Cancer*. 2018;**9**(19):3557-69. [PubMed ID: 30310513]. [PubMed Central ID: PMC6171016]. https://doi.org/10.7150/jca.26350.
19. Ingram H, Dogan M, Eason JD, Kuscu C, Kuscu C. MicroRNAs: Novel Targets in Hepatic Ischemia-Reperfusion Injury. *Biomedicines*. 2022;**10**(4). [PubMed ID: 35453542]. [PubMed Central ID: PMC9028838]. https://doi.org/10.3390/biomedicines10040791.
20. Shi X, Yang H, Birchler JA. MicroRNAs play regulatory roles in genomic balance. *Bioessays*. 2023;**45**(2). e2200187. [PubMed ID: 36470594]. https://doi.org/10.1002/bies.202200187.
21. Olcum M, Tufekci KU, Genc S. MicroRNAs in Genetic Etiology of Human Diseases. *Methods Mol Biol*. 2022;**2257**:255-68. [PubMed ID: 34432283]. https://doi.org/10.1007/978-1-0716-1170-8_13.
22. Hu Y, Luo M. NORAD-sponged miR-378c alleviates malignant behaviors of stomach adenocarcinoma via targeting NRP1. *Cancer Cell Int*. 2022;**22**(1):79. [PubMed ID: 35164743]. [PubMed Central ID: PMC8842946]. https://doi.org/10.1186/s12935-022-02474-5.
23. Nian X, Li L, Ma X, Li X, Li W, Zhang N, et al. Understanding pathogen-host interplay by expression profiles of lncRNA and mRNA in the liver of Echinococcus multilocularis-infected mice. *PLoS Negl Trop Dis*. 2022;**16**(5). e0010435. [PubMed ID: 35639780]. [PubMed Central ID: PMC9187083]. https://doi.org/10.1371/journal.pntd.0010435.
24. Tuergan T, Zhang R, Chen X, Aihemaiti N, Guo X, Ran B, et al. LncRNA Regulation Mechanism in Hepatic Alveolar Echinococcosis with Nanosecond Pulse. *Acta Parasitol*. 2023;**68**(2):420-9. [PubMed ID: 37103765]. https://doi.org/10.1007/s11686-023-00672-3.
25. Martinez-Terroba E, Plasek-Hegde LM, Chiotakakos I, Li V, de Miguel FJ, Robles-Oteiza C, et al. Overexpression of Malat1 drives metastasis through inflammatory reprogramming of the tumor microenvironment. *Sci Immunol*. 2024;**9**(96):eadh5462. [PubMed ID: 38875320]. [PubMed Central ID: PMC12087577]. https://doi.org/10.1126/sciimmunol.adh5462.
26. Mazarei M, Shahabi Rabori V, Ghasemi N, Salehi M, Rayatpisheh N, Jahangiri N, et al. LncRNA MALAT1 signaling pathway and clinical applications in overcome on cancers metastasis. *Clin Exp Med*. 2023;**23**(8):4457-72. [PubMed ID: 37695391]. https://doi.org/10.1007/s10238-023-01179-x.
27. Liao K, Lin Y, Gao W, Xiao Z, Medina R, Dmitriev P, et al. Blocking lncRNA MALAT1/miR-199a/ZHX1 Axis Inhibits Glioblastoma Proliferation and Progression. *Mol Ther Nucleic Acids*. 2019;**18**:388-99. [PubMed ID: 31648104]. [PubMed Central ID: PMC6819876]. https://doi.org/10.1016/j.omtn.2019.09.005.
28. Deping C, Bofan J, Yaogang Z, Mingquan P. microRNA-125b-5p is a promising novel plasma biomarker for alveolar echinococcosis in patients from the southern province of Qinghai. *BMC Infect Dis*. 2021;**21**(1):246. [PubMed ID: 33678159]. [PubMed Central ID: PMC7938541]. https://doi.org/10.1186/s12879-021-05940-z.
29. Cai P, Gobert GN, You H, Duke M, McManus DP. Circulating miRNAs: Potential Novel Biomarkers for Hepatopathology Progression and Diagnosis of Schistosomiasis Japonica in Two Murine Models. *PLoS Negl Trop Dis*. 2015;**9**(7). e0003965. [PubMed ID: 26230095]. [PubMed Central ID: PMC4521869]. https://doi.org/10.1371/journal.pntd.0003965.
30. Xia H, Zhang Z, Yuan J, Niu Q. The lncRNA PVT1 promotes invasive growth of lung adenocarcinoma cells by targeting miR-378c to regulate SLC2A1 expression. *Hum Cell*. 2021;**34**(1):201-10. [PubMed ID: 32960438]. https://doi.org/10.1007/s13577-020-00434-7.